AMCoR
Asahikawa Medical College Repository http://amcor.asahikawa-med.ac.jp/

Journal of Investigative Dermatology. (2005. Feb) 124(2):360-366.

LEKTI is localized in lamellar granules, separated from KLK5 and KLK7, and is secreted in the extracellular spaces of the superficial stratum granulosum

Ishida-Yamamoto, Akemi ; Deraison, Celine ; Bonnart, Chrystelle ; Bitoun, Emmanuelle ; Robinson, Ross ; O'Brien, Timothy J. ; Wakamatsu, Kotaro ; Ohtsubo, Sawa ; Takahashi, Hidetoshi ; Hashimoto, Yoshio ; Dopping-Hepenstal, Patricia J C. ; McGrath, John A. ; Iizuka, Hajime ; Richard, Gabriele ; Hovnanian, Alain

LEKTI is localized in lamellar granules, separated from KLK5 and KLK7, and is secreted in the extracellular spaces of the superficial stratum granulosum

*Akemi Ishida-Yamamoto, †Céline Deraison, †Chrystelle Bonnart, †Emmanuelle Bitoun, ‡Ross Robinson, § Timothy J O'Brien, *Kotaro Wakamatsu,*Sawa Ohtsubo, *Hidetoshi Takahashi, *Yoshio Hashimoto, ¶Patricia JC Dopping-Hepenstal, ¶John A McGrath, *Hajime Iizuka, #Gabriele Richard, and † Alain Hovnanian.

*Department of Dermatology, Asahikawa Medical College, Asahikawa, Japan; †INSERM U563 and Université Paul Sabatier, Department of Genetics, Purpan Hospital, Toulouse, France, ‡Department of Structural Biology, Wellcome Trust Centre for Human Genetics, Oxford, UK, §Department of Obstetrics and Gynecology, University of Arkansas for Medical Science, AR, USA,¶Genetic Skin Disease Group, St John's Institute of Dermatology, GKT Medical school, St Thomas' Hospital, London, UK, and #Department of Dermatology and Cutaneous Biology and the Jefferson Institute of Molecular Medicine, Jefferson Medical College, Philadelphia, PA, USA

Correspondence to: Dr. Akemi Ishida-Yamamoto,
Department of Dermatology, Asahikawa Medical College,
Midorigaoka-Higashi 2-1-1-1, Asahikawa, 078-8510, Japan.
Tel: 81-166-68-2523: Fax: 81-166-68-2529; Email: akemi@asahikawa-med.ac.jp

Short title: LEKTI in Lamellar Granules

Abbreviations: KLK, kallikrein; LG, lamellar granules; NS, Netherton syndrome

Keywords: Electron microscopy; Immunoelectron microscopy; Keratinocytes; Serine protease inhibitor

Summary

LEKTI is a putative serine protease inhibitor encoded by *SPINK5*. It is strongly expressed in differentiated keratinocytes in normal skin but expression is markedly reduced or absent in Netherton syndrome (NS), a severe ichthyosis caused by *SPINK5* mutations. At present, however, both the precise intracellular localization and biological roles of LEKTI are not known. To understand the functional role of LEKTI, we examined the localization of LEKTI together with kallikrein (KLK) 7 and KLK5, possible targets of LEKTI, in human epidermis, by confocal laser scanning microscopy and immunoelectron microscopy. In normal skin, LEKTI, KLK7 and KLK5 were all found in the lamellar granule system, but were separately localized. LEKTI was expressed earlier than KLK7 and KLK5. In NS skin, LEKTI was absent and an abnormal split in the superficial stratum granulosum was seen in three of four cases. Collectively, these results suggest that in normal skin the lamellar granule system transports and secretes LEKTI earlier than KLK7 and KLK5 preventing premature disintegration of cell adhesion. Our data provide fundamental insights into the biological functions of lamellar granules and the pathogenesis of NS.

LEKTI (lympho-epithelial Kazal-type related inhibitor) is a predicted serine protease inhibitor encoded by *SPINK5* (serine protease inhibitor Kazal-type 5), the causative gene of the severe autosomal recessive ichthyotic skin disorder, Netherton syndrome (NS) (Chavanas *et al.*, 2000; Sprecher *et al.*, 2001. 2004; Bitoun *et al.*, 2001). LEKTI is strongly expressed in the granular and uppermost spinous layer of the epidermis (Bitoun *et al.*, 2003). It is processed into short fragments and is secreted from the cells. Among its possible targets are KLK7 (stratum corneum chymotryptic enzyme) and KLK5 (stratum corneum tryptic enzyme). KLK7 and KLK5 are thought to be involved in desquamation through the proteolysis of intercellular adhesion molecules, such as desmoglein (Ekholm *et al.*, 2000). KLK7 is localized in lamellar granules (LG) (Sondel *et al.*, 1995, Ishida-Yamamoto *et al.*, 2004), but ultrastructural localization of KLK5 has not been reported.

NS is characterized by severe ichthyosis (ichthyosis linearis circumflexa and/or congenital ichthyosiform erythroderma), a specific hair-shaft abnormality known as ‘bamboo hair’, and atopic manifestations with high IgE levels. Markedly increased trypsin-like hydrolytic activity has been recently demonstrated in the stratum corneum of NS (Komatsu *et al.*, 2002). This raises the possibility that defective inhibitory regulation of epidermal serine proteases due to decreased LEKTI activity may result in early degradation of desmosomes, and that this might account for the observed skin pathology in NS. Therefore, to elucidate the role of LEKTI in skin biology, we studied the localization of LEKTI, KLK7, and KLK5 in normal human skin by confocal laser scanning microscopy and immunoelectron microscopy and analyzed the structural integrity of the NS epidermis.

Results and Discussion

LEKTI expression was investigated and compared with those of KLK7 and KLK5. The NS patients in this study comprised one individual (case 1) who was a compound heterozygote for the *SPINK5* mutations 377delAT and R790X (Fig 1) similar to an unrelated

previously published case (Bitoun *et al*., 2001), and three cases (cases 2-4) who were all homozygous for the previously described frameshift mutation 2468insA (Chavanas *et al.* 2000). For the skin immunostaining, three different antibodies against LEKTI gave essentially the same results. Concordant with earlier findings, (Bitoun *et al.*, 2003), LEKTI immunoreactivity was detected in normal differentiated epidermal keratinocytes but not in NS epidermis (Figs. 2, 3A, 3B). The observation that no LEKTI protein is detectable on skin biopsy of case 1 (Fig. 3B) indicates that both mutations lead to null alleles. KLK7 and KLK5 have been detected in a thin zone at the border between stratum granulosum and stratum corneum and also in the stratum corneum (Ekholm *et al*. 2000), and this was confirmed by the present study (Fig. 2). Double immunostaining revealed that LEKTI was expressed earlier during epidermal differentiation than KLK7 and KLK5 (Fig. 2). Although immunoelectron microscopy results (see below) showed frequent co-expression of LEKTI and KLKs in the superficial granular cells, a double-positive layer was only occasionally detected by confocal laser scanning microscopy. This may be due to the differences in tissue preparation, penetration of antibodies, epitope masking, and/or sensitivities of techniques. As noted previously (Bitoun *et al.*, 2003), LEKTI staining was concentrated on the apical side of the cells, thus suggesting its association with LG. To evaluate this hypothesis, immunoelectron microscopy was performed.

LG constitute a specialized secretory system within the epidermis. Initially, LG were thought to be isolated granules that migrate to the apical cell surface and secrete their contents into extra-cellular spaces. Recent studies, however, have suggested that LG are part of beaded, tubular structures continuous with the trans-Golgi network (Elias *et al.*, 1988; Norlen, 2001; Ishida-Yamamoto *et al.*, 2004). Ultrastructurally, LG look different depending on the electron microscopy methods used to view them. As shown in Figure 4A, LG are seen as isolated oval-shaped granules in post-embedding methods, while they appear as parts of beaded tubular structures in cryo-ultra microtomy (Fig.4B). For the first time in the present study, we

localized LEKTI within LG using both methods (Fig. 4). Thus, LEKTI has been added to the list of protease inhibitors found in LG that includes elafin and cathepsin D (Pfundt *et al*., 1996, Nakane *et al*., 2002, Ishida-Yamamoto *et al*., 2004), strengthening biological significance of LG in regulation of protease activities. LEKTI labels were aggregated and not evenly distributed throughout the LG system, indicating the heterogeneous nature of the LGs (Ishida-Yamamoto *et al*., 2004). Previous studies have suggested that biologically active fragments derived from LEKTI are released extra-cellularly (Bitoun *et al.*, 2003). As demonstrated for other LG cargoes, LEKTI labels were seen in the extra-cellular spaces in the superficial granular layers and the first cornified layer with release from the apical side of upper granular cells (Fig. 4C). LEKTI immunolabels were also closely associated with the TGN46-positive trans-Golgi network (Fig. 4D). Double labeling with glucosylceramide, a well known LG molecule, showed that each occupies distinct domain of beaded tubular structure (Fig 4E). This separate localization of different cargoes was maintained up to the undersurface of the plasma membrane in the stratum granulosum-stratum corneum interface.

The ultrastructural localization of LEKTI was compared with that of KLK7. As reported previously (Ishida-Yamamoto *et al.*, 2004; Sondell *et al*., 1995), KLK7 was localized in the LG system (Figs. 5, 6) but was not co-localized with LEKTI within keratinocytes. Indeed, in the double-positive cells, LEKTI and KLK7 localized separately within the LG system (Fig. 6). Consistent with the immunofluorescent results, LEKTI was detected intracellularly and extracellularly in deeper epidermal layers than KLK7, which was found in more superficial differentiated keratinocytes (Fig. 5). This finding suggests that LEKTI is expressed and released earlier than its target proteases, which is consistent with a role in preventing premature proteolysis of extracellular matrix proteins or cell surface adhesion molecules, and in controlling the timing of desquamation. In the stratum granulosum-stratum corneum interface, LEKTI and KLK7 were found either separately or mixed together (Fig. 7). About 70% of LEKTI gold labels (49 out of 66) were within 30 nm distance from the nearest

KLK7 labels. Above the first layer of the stratum corneum, LEKTI immunoreactivity was not detected, but KLK7 labels remained up to the superficial layers. Future biochemical analysis of stratum corneum will be needed to define when LEKTI-derived fragments and their enzymatic activities are lost in the stratum corneum.

We also studied ultrastructural localization of KLK5 and found it in the LG system (Fig. 8) and extra-cellular spaces between granular cells and cornified cells. Double labeling showed that LEKTI and KLK5 occupied distinct domain of the LG system (Fig. 8B). The separate transport of LEKTI and KLKs may prevent their interaction within the cells. However, this speculation based on microscopy has to be evaluated by other methods such as biochemical analysis of purified proteins.

On light microscopy, the stratum corneum of NS skin was thick and laminated, and the intercellular clefts were observed from just above the stratum granulosum (Fig. 3C). Although this lamination has often been thought to be an artifact that arises during tissue dehydration with ethanol, we hypothesized that NS skin might actually be more vulnerable and easily separated as part of a real pathological process. In Epon-embedded electron microscopy samples, inter-cellular micro-splits were observed in the superficial granular layer in three of four NS cases (cases 1 to 3) (Fig. 9). The splits were associated with asymmetrical separation of desmosomes and intercellular release of lamellar granule contents, including KLK7 (Figs. 9 and 10). KLK7 was localized in the LG system in NS as in normal skin and was seen around desmoglein 1 labels at desmosomal split in NS (Figs. 10B, and 10C). (KLK5 localization in NS could not be investigated, because NS skin samples were processed for a post-embedding method only and the antibody did not work.) We believe that these abnormalities are distinctive microscopic features of NS, which indicate that the loss of adhesion within the stratum corneum is a key pathological event in this genodermatosis. Recent observations in *SPINK5*-null mice seem to support this notion (Descargues *et al*. 2004, submitted). Micro-split in the stratum corneum were frequently observed in the stratum

corneum in the normal as well as in NS skin, but granular cell splits were not found in 20 normal control skin samples. Previously reported electron microscopic examinations of NS have found various morphological changes, including premature secretion of LG contents, and abnormal extracellular material in the stratum corneum (Fartasch *et al.*, 1999). Premature detachment or entirely missing stratum corneum has also been documented (De Wolf et al., 1996, Hausser and Anton-Lamprecht, 1996). Micro-clefts found in the stratum granulosum of NS are likely to be one of the primary consequences of premature protease activation.

Appropriate coordination of proteases and their inhibitors is vital for proper desquamation, which requires the proteolytic dissolution of intercellular cohesive structures in the stratum corneum. Clinically, sheet-like peeling of the stratum corneum resembling peeling skin syndrome has been observed in NS patients (Sprecher *et al.*, 2001). Although the actual physiologic substrates of LEKTI are currently unknown, these clinical symptoms together with the present demonstration of split desmosomes strongly suggests that LEKTI is a specific inhibitor of proteases involved in desmosome disintegration. Allen *et al.* proposed the pathogenic sequence model in NS, where increased tryptic enzyme leads to barrier defects via multiple pathways including activation of phospholipase A2, activation of IL-1α, and desmosomal degradation (Allen *et al.* 2001). Komatsu *et al*. found a marked increase in trypsin-like hydrolytic activity in stratum corneum from NS, and proposed a model for the proteolytic processing of LEKTI in the epidermis and inhibitory regulation of corneocyte desquamation by a set of LEKTI–derived peptides (Komatsu *et al*., 2002). The present results support this model and provide further fundamental information about the biological roles of LEKTI.

Materials and Methods

Patients and clinical material

Case 1 was a 17-year-old Japanese girl with generalized congenital ichthyosiform

erythroderma, who was born of to non-consanguineous parents. She was initially diagnosed as having non-bullous congenital ichthyosiform erythroderma (Hashimoto *et al.*, 1987). Skin lesions improved with age, but the face and trunk were constantly erythematous and scaly plaques remained in the extremities. Marked growth retardation was noted at the age of 3 years. Hair abnormalities were noted after puberty. Hair did not grow long and trichorrhexis nodosa was detected in some hair shafts. Serum IgE levels were elevated (3857 IU/ml). Cases 2 to 4 were typical NS cases from Kashmir corresponding to affected members of families 11, 12 and 13 in the previous report (Chavanas *et al.*, 2000). Tissue samples of normal skin were used as controls. All participants gave informed consent and the protocol was approved by the institutional ethics review boards. The study was conducted according to the principles of the Helsinki declaration.

Antibodies

The primary antibodies were three LEKTI antibodies (rabbit polyclonal antibodies against N-terminal D1-D6 domains (Bitoun *et al.*, 2003), mouse monoclonal antibodies against D1-D6 domains (Bitoun *et al.*, 2003) and rabbit polyclonal antibodies against D8-D11 domains (Hovnanian, unpublished)), mouse anti-Desmoglein 1 (Dsg1-P23, Progen, Heidelberg, Germany), rabbit polyclonal anti-KLK7 (Tanimoto *et al*, 1999), rabbit polyclonal anti-KLK5 (Santa Cruz Biotechnology, Santa Cruz, Calif.), sheep anti-TGN46 (Serotec, Oxford, UK) and rabbit anti-glucosylceramides (Glycobiotech, Kukels, Germany).

For immunofluorescence analysis, the following secondary reagents were used: Alexa-Fluor 488 goat anti-rabbit IgG highly cross-absorbed (Molecular Probes, Eugene, OR) and Cy3-labeled goat anti-mouse IgG (Amersham Bioscience, Buckinghamshire, UK). Secondary antibodies used for electron microscopy were 10 nm or 5 nm gold-conjugated goat anti-rabbit IgG (Amersham Bioscience, BBInternational, Cardiff, UK), 10 nm or 5nm gold-conjugated goat anti-mouse IgG (Amersham Bioscience) and 10 nm gold-conjugated donkey anti-sheep

IgG (BBInternational).

Immunostaining and morphological analysis

Immunofluorescence analysis was performed as described previously (Ishida-Yamamoto *et al*., 2004). Fluorescence images were obtained using a Fluoview FV500 confocal laser scanning microscope (Olympus America Inc., Melville, New York). For immunohistochemistry, a standard streptavidin-biotin method using diaminobenzidine as a substrate for peroxidase was employed on formalin-fixed and paraffin-embedded sections of skin samples from case 1. Immunoelectron microscopy using Lowicryl K11M resin- and HM20 resin-(Chemische Werke Lowi, Waldkraiburg, Germany) embedded samples and ultrathin cryosections was performed as described previously (Ishida-Yamamoto *et al*., 2004). For all immunohistochemistry, negative controls included incubation in the presence of secondary antibody alone and incubation with unrelated primary antibodies.

For conventional transmission electron microscopy, small pieces of skin samples were fixed in half-strength Karnovsky fixative, followed by further fixation in 1% osmium tetroxide in distilled water. After en bloc staining with uranyl acetate, specimens were dehydrated in ethanol and embedded in Epon812 (Taab, Berkshire, UK). Ultrathin sections were stained with uranyl acetate and lead citrate.

Mutation analysis

With informed consent, genomic DNA was extracted from a peripheral blood sample of patient 1 and used to amplify the entire coding sequence and flanking non-coding sequences of the *SPINK5* gene by polymerase chain reaction (PCR). All 33 coding exons were separately amplified, gel purified and subjected to bi-directional direct DNA sequence analysis as previously described (Sprecher *et al*. 2001). Sequence variants were confirmed in the patient and excluded from control alleles by dHPLC analysis on a Wave DNA fragment analysis

system (Transgenomics, Omaha, NE) (mutation in exons 5; 90 control individuals) and by restriction fragment analysis with *Taq*I (mutation in exon 25; 30 control individuals). For the former, 10 µl of each sample were separately injected and analyzed over 7.5 min at a non-denaturing temperature of 50°C to determine the amplicons sizes. For restriction enzyme analysis, 400 bp amplicons encompassing exon 25 were purified on MicroSpin S-400 columns (Amersham Pharmacia Biotech, Priscataway, NJ), digested for 2 h at 37° C according to the supplier's recommended conditions (New England Biolabs), and separated on 2% agarose gels. Since the mutation 2368C->T destroys a TaqI recognition site, the 367 bp band remained intact in the presence of the mutation, while the wildtype sequence was cleaved in a 181 bp and a 186 bp fragment, which were visible as a single broad band (Fig. 1).

Acknowledgments

We would like to thank Mrs. Keiko Nishikura and Miss Yasuyo Nishinome for their valuable technical assistance. This work was supported by grants from the Ministry of Education, Culture, Sports, Science and Technology and the Ministry of Health, Labor and Welfare of Japan to A. I-Y. Electron microscopy samples were observed at the Electron Microscopy Unit of the Central Laboratory for Research and Education at Asahikawa Medical College. Molecular studies were supported by NIH grants AR47157 and AR02141 to G. R. LEKTI antibodies purification and characterization were supported by PHRC grant 102908 and INSERM/AFM/Ministry of Research grant A00080BS to A.H.

Figure legends

Figure 1

Mutations of the SPINK5 gene identified in Case 1. Sequence chromatograms illustrate a heterozygous transition (2368C/T) in exon 25 leading to amino acid replacement R790X (A, left) compared to the wildtype sequence (A, right). The mutation results in loss of a *Taq*I site and prevents digestion of the mutant sequence. *Taq*I restriction fragment analysis of a PCR amplicon of exon 25 from the affected patient (P) results in 2 bands, which represent the undigested fragment (367 bp) of the mutant allele in addition to the cleaved fragments (181 bp and 186 bp, both appear as one band) of the wildtype allele. In contrast, amplicons of 6 normal controls (C1-C6) show complete digestion. M: DNA 100bp ladder (Promega, WI). Figure 1B illustrates a heterozygous 2-base pair deletion in exon 5 (377delAT) resulting in frameshift and a premature termination codon (B, top left). The mutant sequence of exon 5 is 2 nucleotides shorter than the wildtype sequence (B, bottom right) as evident from the second peak of the HPLC profile (B, top right) compared to normal (B, bottom right).

Figure 2

LEKTI is expressed earlier than kallikrein (KLK) 7 (A) and KLK5 (B) in the epidermis. LEKTI staining (mouse monoclonal antibody, seen in red) is expressed from the upper spinous layer, while KLK7 and KLK5 are detected in the most superficial granular cells (green). A double-positive zone is seen in between (orange arrows). Note the apical localization of LEKTI (white arrows). Straum corneum is positive to both KLKs, but negative to LEKTI. Confocal laser scanning microscopy. Differential interference microscopy images are superimposed upon immunofluorescent images.

Figure 3

LEKTI is deficient and cornified cells are less adhesive in Netherton syndrome (NS). Immunohistochemical staining using a polyclonal antibody against the D1-D6 domains of LEKTI revealed the presence of LEKTI protein in the apical parts of the spinous and granular cells of normal skin (A), but not in the NS skin (Case 1) (B). Using hematoxylin-eosin staining of paraffin-embedded sections, the stratum corneum was found to be thickened in NS (Case 1) (C) than in normal skin (D). In NS, the outlines of the cells were undulated and extensive clefts were noted starting in the deeper layer, as indicated by the arrow, in contrast to the smooth outlines of normal stratum corneum.

Figure 4

LEKTI is transported through the lamellar granule system. Post-embedding immunoelectron microscopy using Lowicryl HM20 resin (A, D) and a cryo-ultra microtomy method (B, C, E). (A, B) LEKTI signals (black arrows) are detected in the lamellar granules using polyclonal antibodies against D8-D11 in A and D1-D6 in B. Note that lamellar granules are seen as isolated granules in the post-embedding method (A), but appear as beaded tubular structures in the cryo-ultra microtomy (B). Lamellar internal structures are seen in both methods (white arrows). (C) LEKTI is secreted from the apical side of upper granular cells (arrows). d, desmosomes. Polyclonal antibody to D8-D11 and desmoglein 1 monoclonal antibody were used and were labeled with 5 and 10 nm immunogold, respectively. (D) LEKTI antibody to D8-D11 labels are closely associated with those of the TGN46-positive trans-Golgi network. (E) LEKTI (monoclonal antibody, 5 nm gold labels) and glucosylceramides (GlcCer, 10 nm gold labels) are localized within the same continuous beaded tubular structure of lamellar granule system.

Figure 5

LEKTI is secreted earlier than kallikrein (KLK) 7. (A) shows a lower magnification view of the stratum corneum (SC), the most superficial stratum granulosum (SG1), the second (SG2) and

the third granular layer (SG3). The rectangular area marked as 'B' is shown at higher magnification in Figure 5B, which shows LEKTI secreted into the extra-cellular spaces (ECS) between SG2 and SG3. Figure 5C is a higher magnification view of the boxed area marked 'C' in Figure 5B showing KLK7-containing lamellar granules in SG2. d, desmosomes. Cryo-ultra microtomy method. A monoclonal antibody to LEKTI D1-D6 and a polyclonal KLK7 antibody were used and were labeled with 10 and 5 nm immunogold, respectively.

Figure 6

LEKTI and kallikrein (KLK) 7 are transported separately in the lamellar granule system. (A) shows a lower magnification view of the most superficial stratum granulosum (SG1), the second (SG2) and the third stratum granulosum (SG3) and the most superficial stratum spinosum (SS). The marked rectangular area in SG3 is shown at higher magnification in Figure 6B. Cryo-ultra microtomy method. A monoclonal LEKTI antibody to D1-D6 and a polyclonal KLK7 antibody were used and were labeled with 10 and 5 nm immunogold, respectively.

Figure 7

LEKTI and kallikrein (KLK) 7 are co-localized in the extra-cellular spaces (ECS). In the ECS of the stratum granulosum (SG1)-stratum corneum (SC) interface, LEKTI (5 nm gold labels, small arrows) and KLK7 (10 nm gold labels, large arrows) can be seen separated in some places, but are apparently co-localized in others.

Figure 8

Kallikrein (KLK) 5 is localized in the lamellar granule system, but separated from LEKTI. (A) Note beaded tubular structure with partial lamellar internal structures (white arrows) of the lamellar granule system containing KLK5 as aggregates (black arrows). (B) shows LEKTI (10 nm gold) and KLK5 (5 nm gold) double labeling. Cryo-ultramicrotomy method.

Figure 9

Early desmosome split in Netherton syndrome (NS). By conventional transmission electron microscopy, a desmosomal split is seen in the superficial granular cells (A, B). The rectangular area marked in Figure A is shown at higher magnification in Figure B. Note that the midline structures of the desmoglea remain on the basal side of split desmosomes (d) (arrows in B). Using desmoglein 1 immunoelectron microscopy, immunolabeling is detected in the desmoglea in the basal part of the split desmosome in NS (arrow, C), and intact desmosomes in normal control skin (D) (post-embedding method). Asterisks indicate lamellar granule contents secreted into the extra-cellular spaces.

Figure 10

Desmosome disintegration coincides with kallikrein (KLK) 7 secretion. (A) In the lower stratum corneum where KLK7 labels (5 nm gold) are detected in the intercellular spaces, desmoglein 1 (DSG1) (10 nm gold) labels are associated with intact desmosomes in the normal skin. (B) In Netherton syndrome skin, the early sign of desmosomal split is detected (right hand side). Note the many KLK7 labels around DSG1 labels. KLK7 and DSG1 double immunolabeling. (C) A KLK7 positive lamellar granule found in Netherton syndrome skin. Post-embedding immunoelectron microscopy.

References

Allen A, Siegfried E, Silverman R, *et al*: Significant absorption of topical tacrolimus in 3 patients with Netherton syndrome. Arch Dermatol 137: 747-750, 2001

Bitoun E, Chavanas S, Irvine AD, *et al*.: Netherton syndrome: disease expression and spectrum of SPINK5 mutations in 21 families. J Invest Dermatol 118: 352-361, 2001

Bitoun E, Micheloni A, Lamant L, *et al*.: LEKTI proteolytic processing in human primary keratinocytes, tissue distribution and defective expression in Netherton syndrome. Hum Mol Genet 12: 2417-2430, 2003

Chavanas S, Bodemer C, Rochat A, *et al*.: Mutations in SPINK5, encoding a serine protease inhibitor, cause Netherton syndrome. Nature Genetics 25: 141-142, 2000

De Wolf K, Ferster A, Sass U, Andre J, Stene J-J, Song M: Netherton's syndrome: a severe neonatal disease. Dermatology 192: 400-402, 1996

Ekholm IE, Brattsand M, Egelrud T: Stratum corneum tryptic enzyme in normal epidermis: a missing link in the desquamation process? J Invest Dermatol 114: 56-63, 2000

Elias PM, Cullander C, Mauro T, Rassner U, Komuves L, Brown BE, Menon GK: The secretory granular cell: the outermost granular cell as a specialized secretory cell. J Invest Dermatol Dermatology Symposium Proceedings 3:87-100, 1998.

Fartasch M, Williams ML, Elias PM: Altered lamellar body secretion and stratum corneum membrane structure in Netherton syndrome. Arch Dermatol 135: 823-832, 1999

Hashimoto Y, Ishida A, Matsumoto M, Iizuka H, Mizumoto T, Murono K, Fujita K: A case of nonbullous congenital ichthyosiform erythroderma. Japanese Journal of Clinical Dermatology 41: 207-213, 1987

Hausser I, Anton-Lamprecht I: Severe congenital generalized exfoliative erythroderma in newborns and infants: a possible sign of Netherton syndrome. Pediatr Dermatol 13: 183-199, 1996

Ishida-Yamamoto A, Simon M, Kishibe M, *et al*.: Epidermal lamellar granules transport

different cargoes as distinct aggregates. J Invest Dermatol 122: 1137-1144, 2004

Komatsu N, Takata M, Otsuka N, Ohka R, Amano O, Takehara K, Saijoh K: Elevated stratum corneum hydrolytic activity in Netherton syndrome suggests an inhibitory regulation of desquamation by SPINK5-derived peptides. J Invest Dermatol 118: 436-443, 2002

Nakane H, Ishida-Yamamoto A, Takahashi H, Iizuka H: Elafin, a secretory protein, is cross-linked into the cornified cell envelopes from the inside of psoriatic keratinocytes. J Invest Dermatol 119: 50-55, 2002

Norlen L: Skin barrier formation: the membrane folding model. J Invest Dermatol 117: 823-829, 2001

Pfundt R, van Ruissen F, van Vlijmen-Willems IMJJ, *et al*. Constitutive and inducible expression of SKALP/elafin provides anti-elastase defense in human epithelia. J Clin Invest 98: 1389-1399, 1996

Sondell B, Thornell L-E, Egelrud T: Evidence that stratum corneum chymotryptic enzyme is transported to the stratum corneum extracellular space via lamellar bodies. J Invest Dermatol 104: 819-823, 1995

Sprecher E, Chavanas S, DiGiovanna JJ, *et al*.: The spectrum of pathogenic mutations in SPINK5 in 19 families with Netherton syndrome: implications for mutation detection and first case of prenatal diagnosis. J Invest Dermatol 117: 179-187, 2001

Sprecher E, Tesfaye-Kedjela A, Ratajczak P, Bergman R, Richard G: Deleterious mutations in SPINK5 in a patient with congenital ichthyosiform erythroderma: molecular testing as a helpful diagnostic tool for Netherton syndrome. Clin Exp Dermatol, 2004, in press.

Tanimoto H, Underwood LJ, Shigemasa K, Yan Y, Clarke J, Parmley TH, O'Brien TJ: The stratum corneum chymotryptic enzyme that mediates shedding and desquamation of skin cells is highly overexpressed in ovarian tumor cells. Cancer 86:2074-2082, 1999.

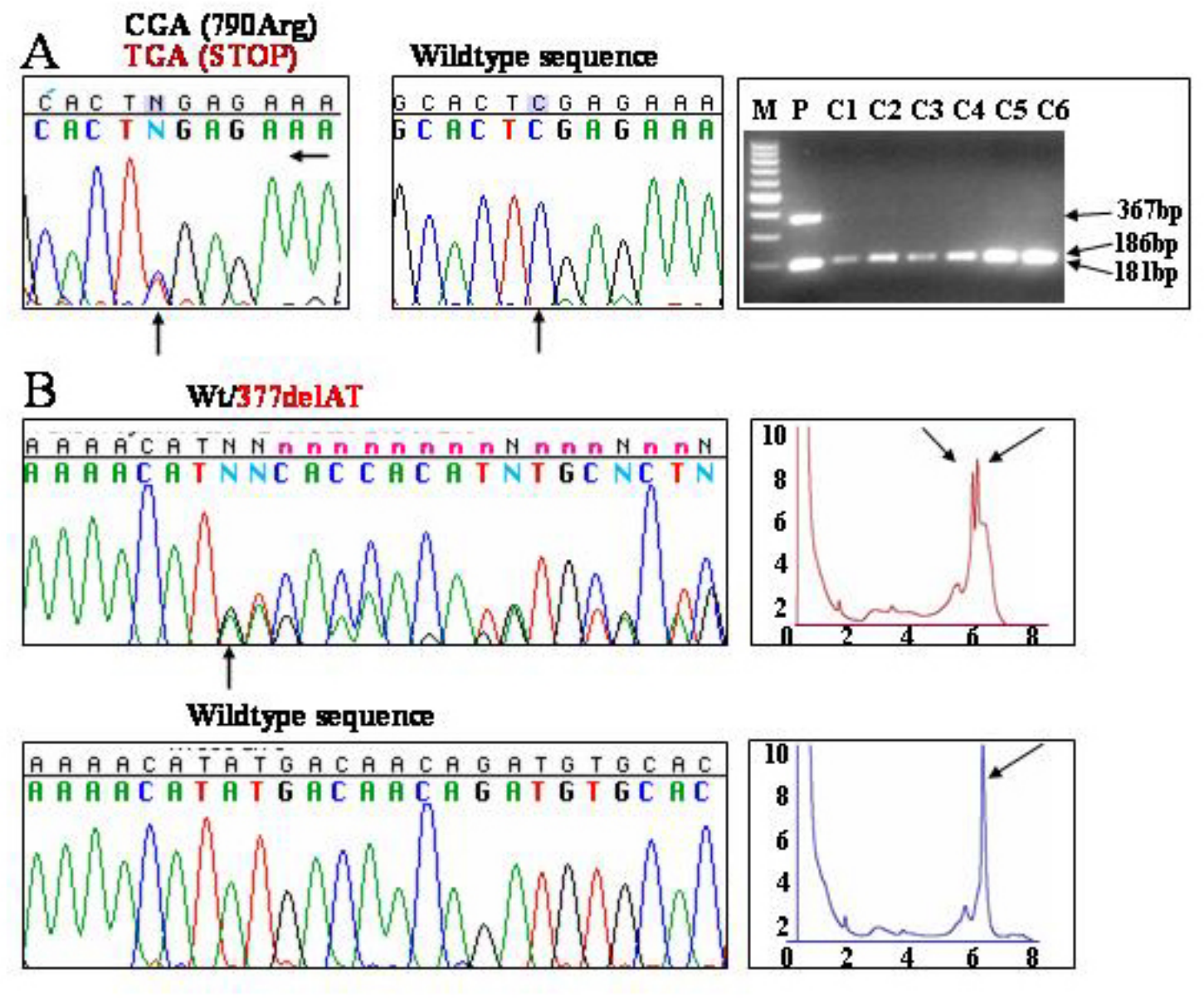
A
CGA (790Arg)
TGA (STOP)
Wildtype sequence
M P C1 C2 C3 C4 C5 C6
367bp
186bp
181bp
B
Wt/377delAT
Wildtype sequence

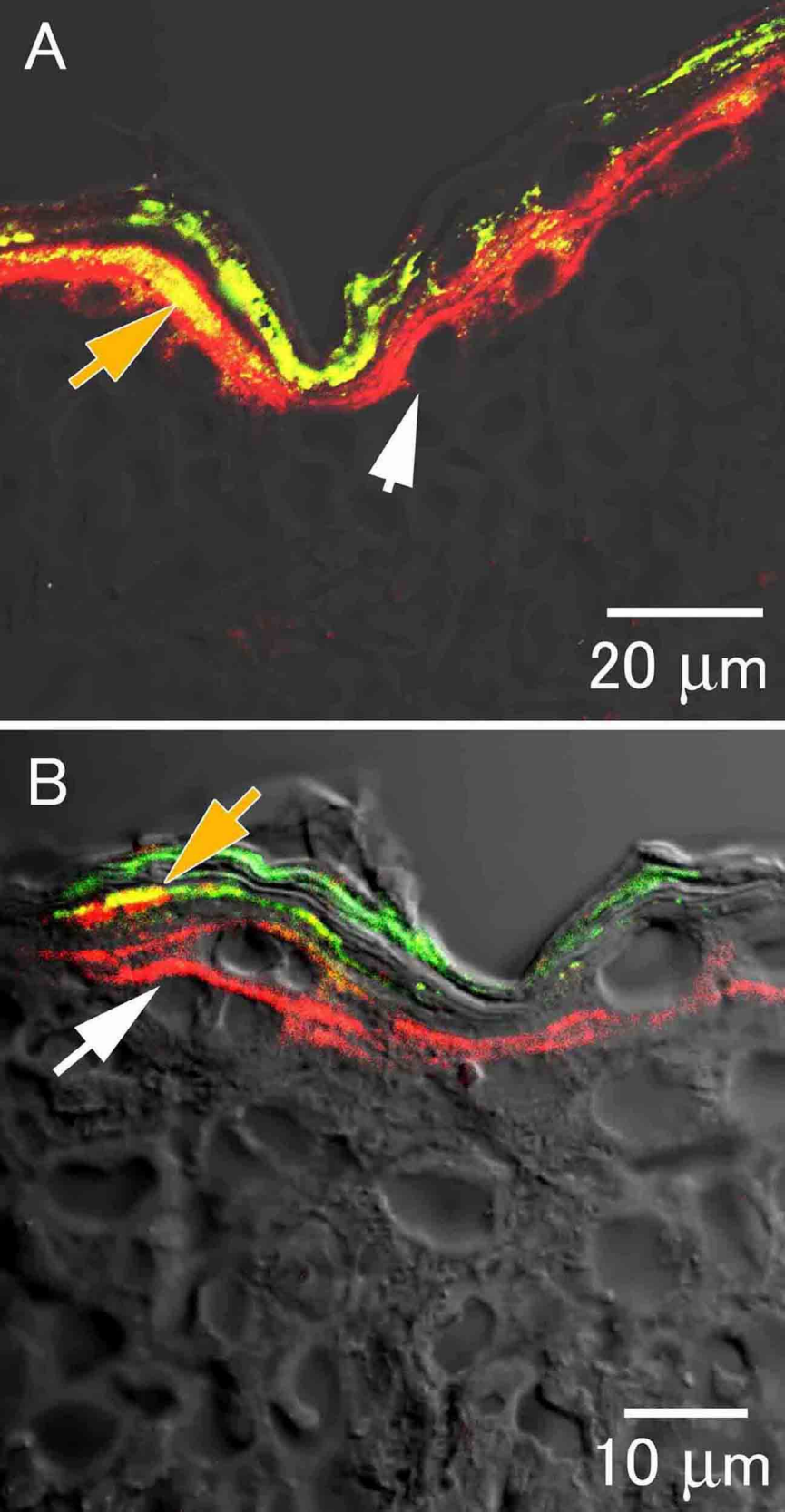
A
20 µm
B
10 µm

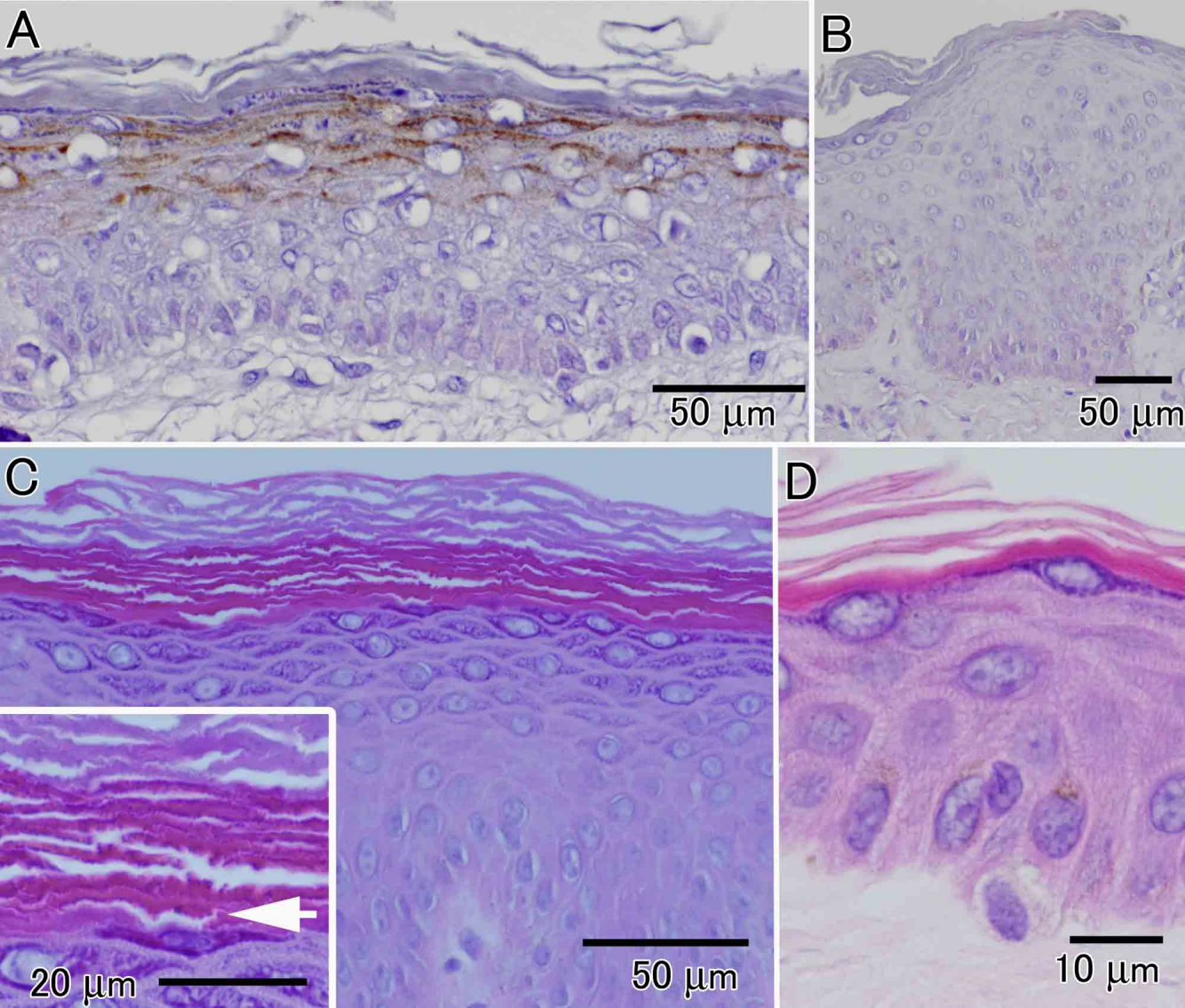
A
50 µm
B
50 µm
C
20 µm
50 µm
D
10 µm

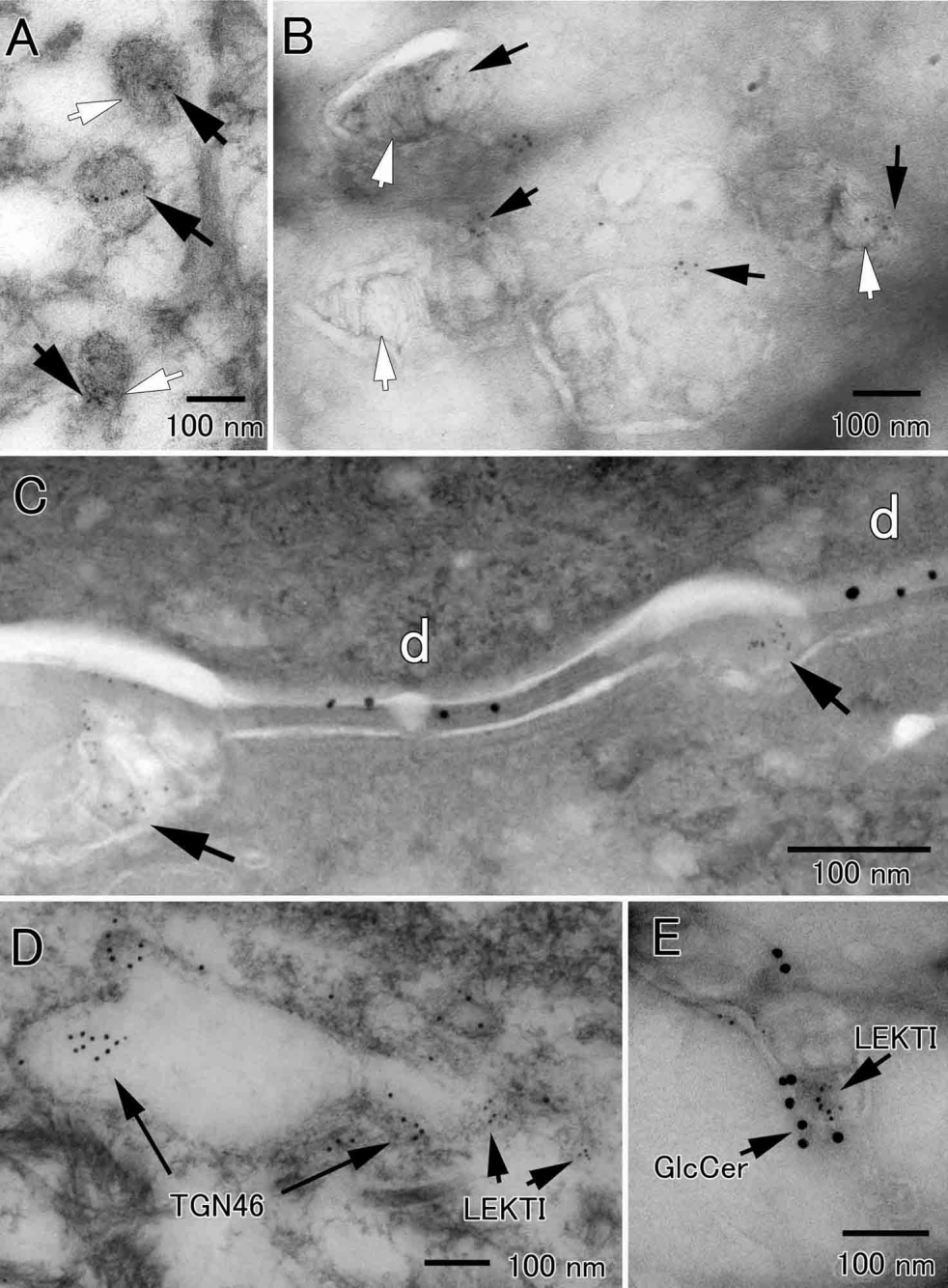
A
100 nm
B
100 nm
C
d
d
100 nm
D
TGN46
LEKTI
100 nm
E
LEKTI
GlcCer
100 nm

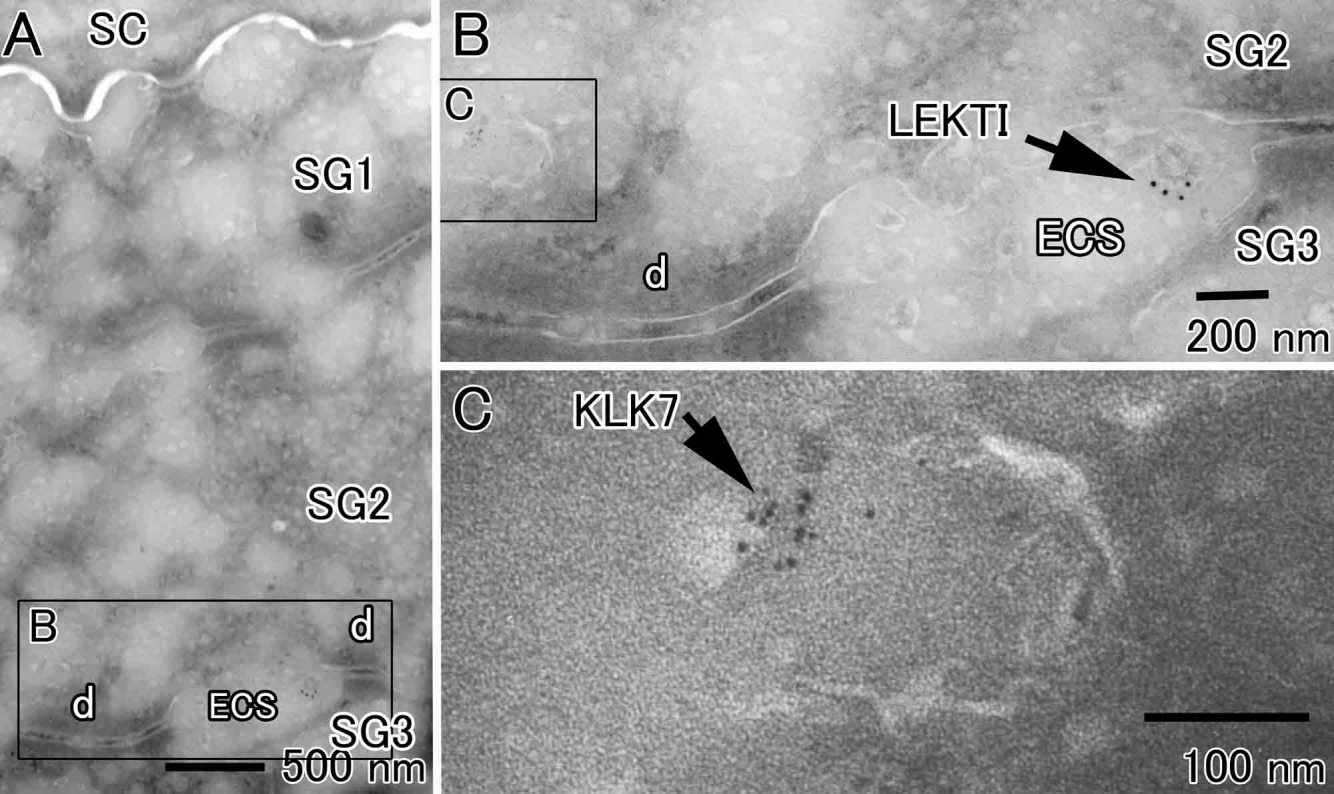
A
SC
SG1
SG2
B
d
d
ECS
SG3
500 nm
B
C
SG2
LEKTI
ECS
SG3
d
200 nm
C
KLK7
100 nm

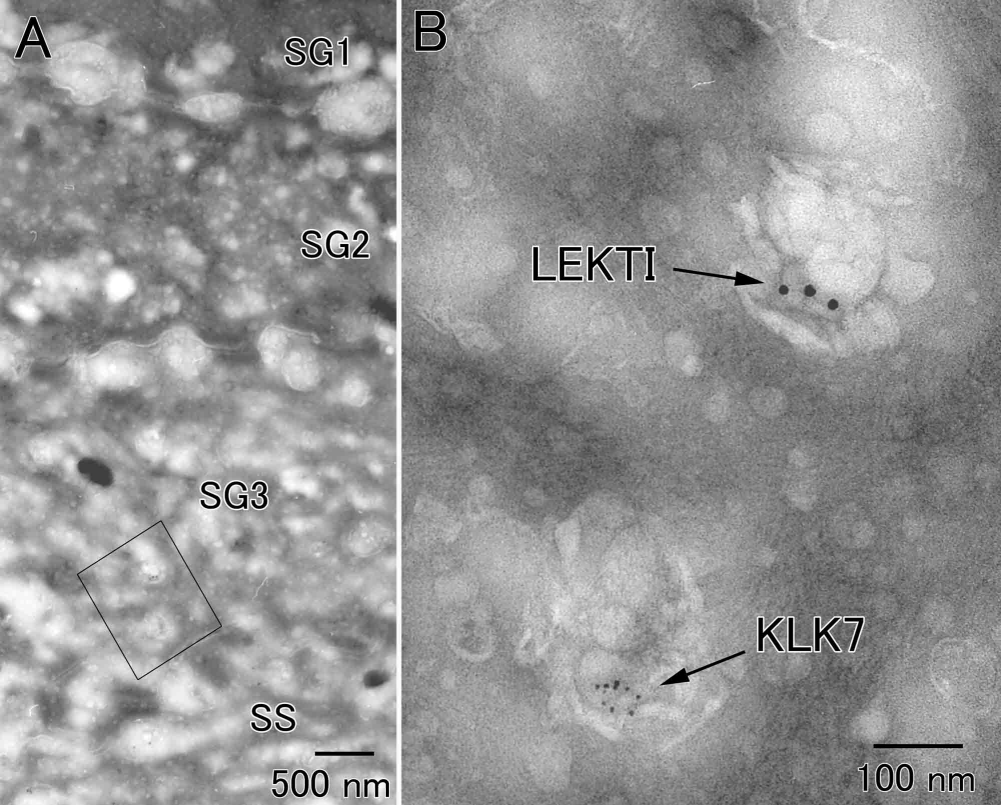
A
SG1
SG2
SG3
SS
500 nm
B
LEKTI
KLK7
100 nm

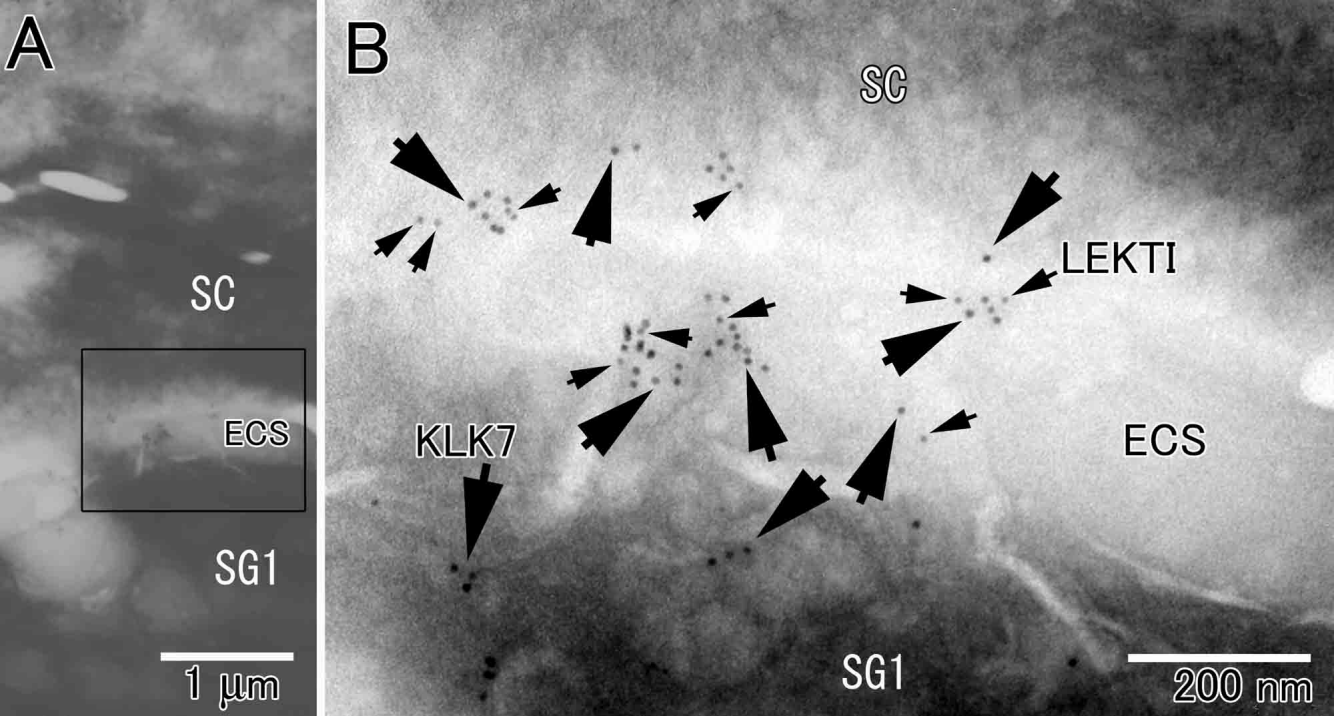
A
SC
ECS
SG1
1 μm
B
SC
LEKTI
KLK7
ECS
SG1
200 nm

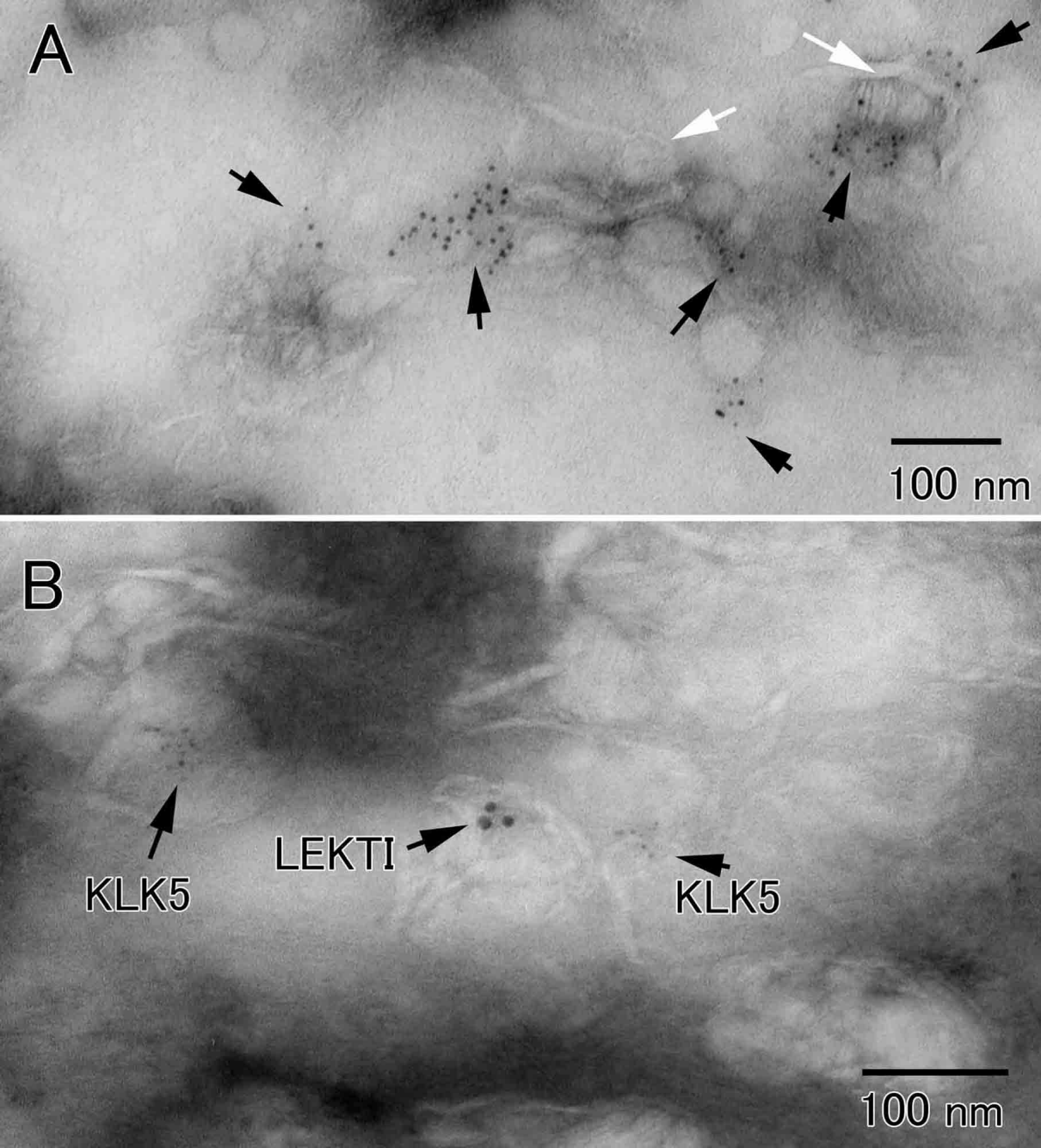
A
100 nm
B
KLK5
LEKTI
KLK5
100 nm

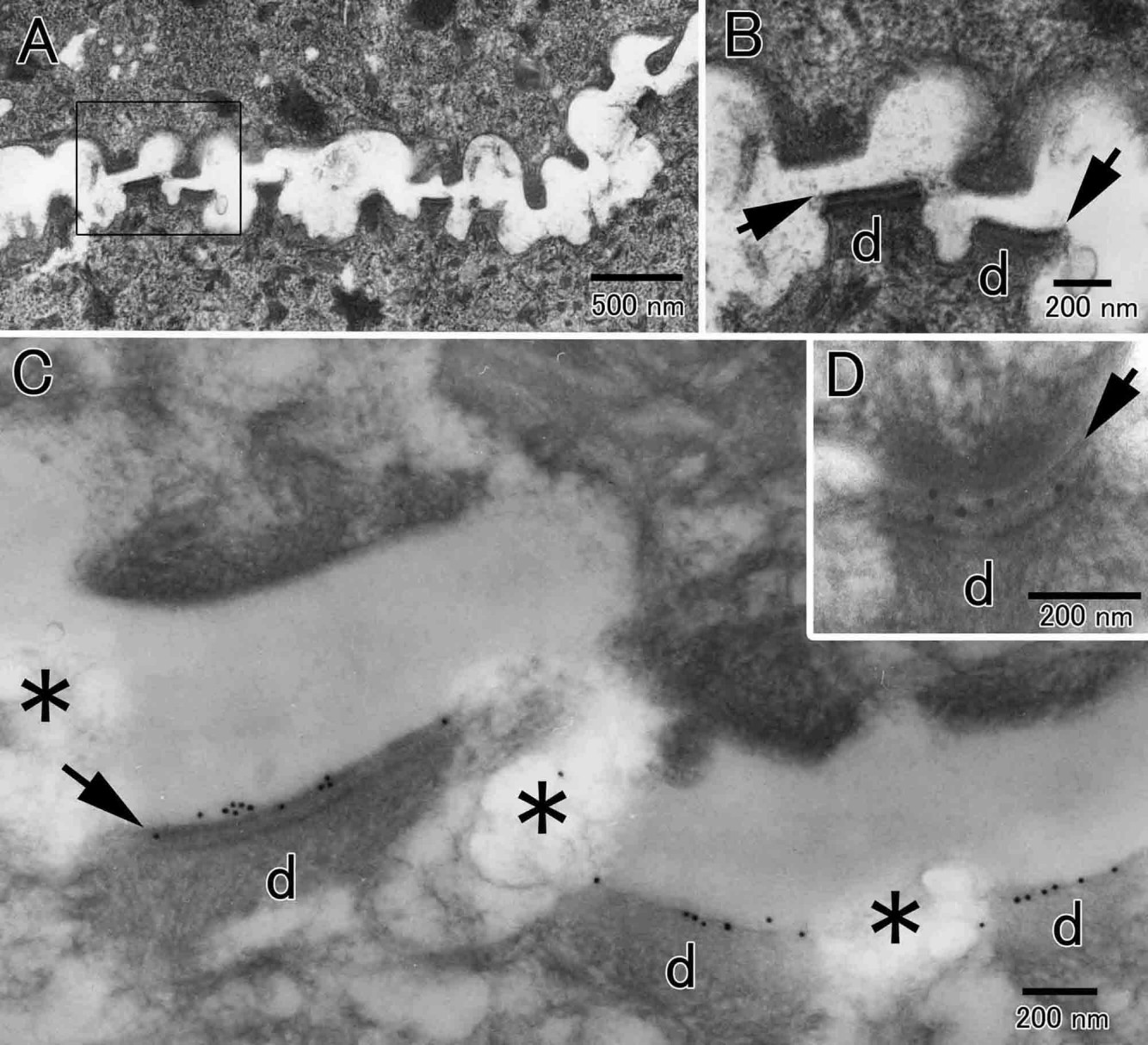
A
500 nm
B
d
d
200 nm
C
*
*
*
d
d
d
D
d
200 nm
200 nm

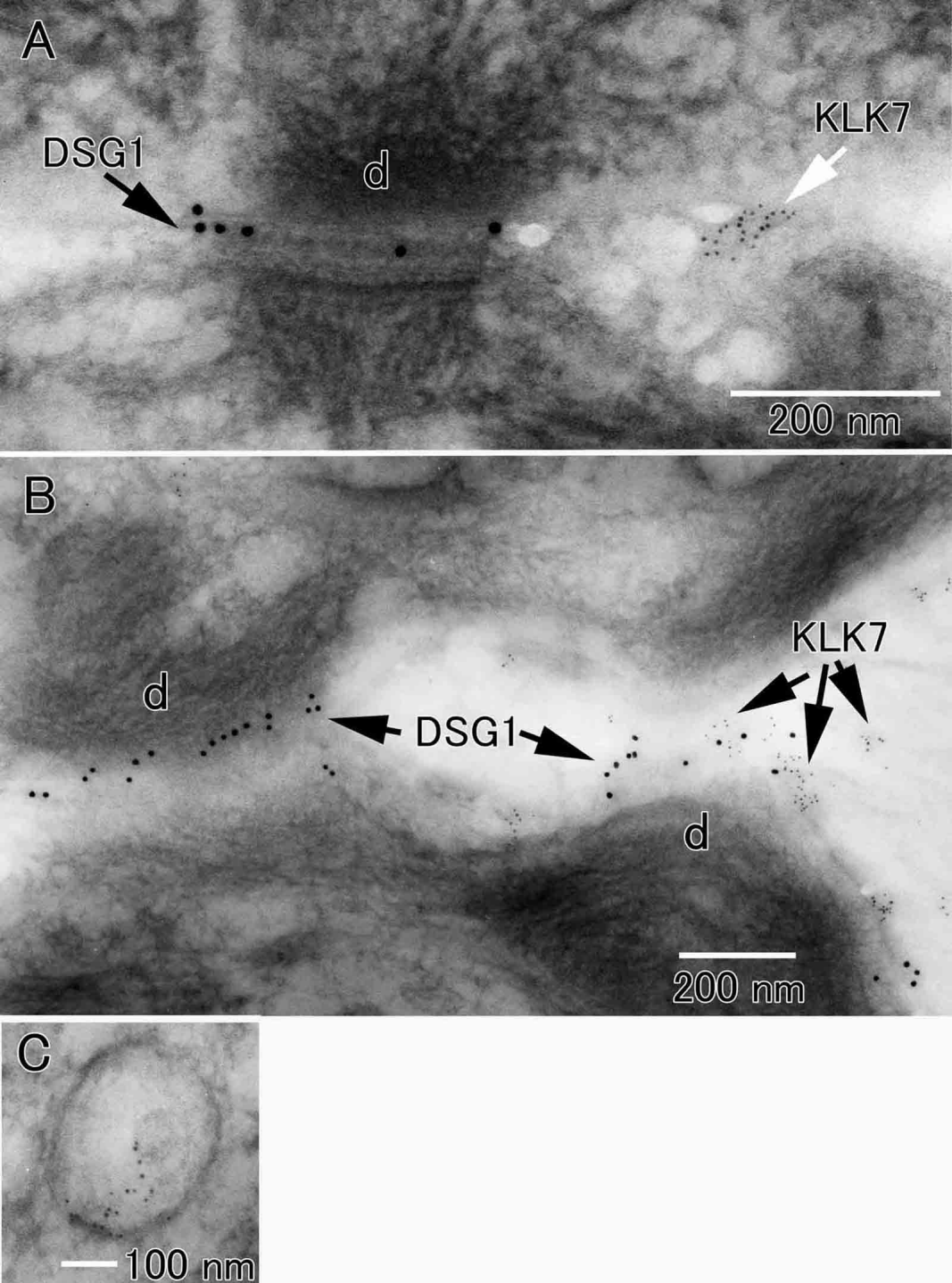
A
DSG1
d
KLK7
200 nm
B
d
DSG1
KLK7
d
200 nm
C
100 nm